Progressive Bundling of Fibrillin Microfibrils Into Oxytalan Fibers in the Chick Presumptive Dermis

ARTICLE *in* THE ANATOMICAL RECORD ADVANCES IN INTEGRATIVE ANATOMY AND EVOLUTIONARY BIOLOGY · JANUARY 2013

Impact Factor: 1.54 · DOI: 10.1002/ar.22619 · Source: PubMed

Progressive Bundling of Fibrillin Microfibrils Into Oxytalan Fibers in the Chick Presumptive Dermis

KEIZO SHINOZUKA,[1] YOSUKE YAMAZAKI,[1,2,3] MAKI YUGUCHI,[1,2] TAKU TORIUMI,[1,3] RIE SUZUKI,[3] EICHI TSURUGA,[4] AND KEITARO ISOKAWA[1,2,3]*

[1]Department of Anatomy, Nihon University School of Dentistry, Tokyo, Japan
[2]Division of Functional Morphology, Dental Research Center, Nihon University School of Dentistry, Tokyo, Japan
[3]Department of Oral Structure and Function, Nihon University Graduate School of Dentistry, Tokyo, Japan
[4]Section of Functional Structure, Department of Morphological Biology, Division of Biomedical Sciences, Fukuoka Dental College, Fukuoka, Japan

ABSTRACT

Dorsoventral fibers in the presumptive dermis of the chick limb bud reported first by Hurle's group in 1989 are now revealed as bundles of fibrillin microfibrils (Isokawa et al., 2004). The bundles, which could be called oxytalan fibers at the light microscopic level, are aligned perpendicularly to the overlying ectoderm and form a unique fiber array, originating directly from the basal lamina. This well-oriented organization is beneficial in examining the process of *in vivo* bundling of microfibrils into oxytalan fibers. In this study, sections through the presumptive limb dermis were preferentially prepared from chick embryos at Days 4–6 (ED4-6). Immunohistochemically, fibrillin-positive dots representing cross-sectioned surfaces of individual fibers, increased in size from ED4 to 6, but their number per unit area remained constant. Ultrastructurally, a single oxytalan fiber at ED4 consisted of ~15 microfibrils; the latter number increased fourfold from ED4 to 5 and threefold from ED5 to 6. Oxytalan fibers were all closely associated with mesenchymal cell; notably, the fibers at ED5 and 6 were held in a shallow ditch on the cell body or by lamellipodial cytoplasmic protrusion. In the sites of cell–fiber adhesion, microfibrils in the periphery of an oxytalan fiber appeared to adhere directly or by means of short flocculent strands to a nearby cell membrane; the latter showed a thickening of plasmalemma and its undercoat, indicating the presence of adhesive membrane specification. These findings suggest that the bundling of microfibrils is a progressive and closely cell-associated process. Anat Rec, 296:71–78, 2013. ©2012 Wiley Periodicals, Inc.

Key words: microfibril; fibrillin; oxytalan fiber; bundle formation

Keizo Shinozuka and Yosuke Yamazaki contributed equally to this work.

Grant sponsors: Sato Fund; Dental Research Center at Nihon University School of Dentistry; Advanced Science Research Center at Fukuoka Dental College; The Promotion and Mutual Aid Corporation for Private Schools of Japan; Grants-in-Aid for Scientific Research from the MEXT of Japan.

*Correspondence to: Keitaro Isokawa, DDS, PhD, Department of Anatomy, Nihon University School of Dentistry, 1-8-13 Kanda-Surugadai, Chiyoda-ku, Tokyo 101-8310, Japan. Fax: +81-3-3295-8783. E-mail: isokawa.keitaro@nihon-u.ac.jp

Received 20 August 2012; Accepted 21 September 2012.

DOI 10.1002/ar.22619

Published online 15 November 2012 in Wiley Online Library (wileyonlinelibrary.com).

Extracellular architectural molecules such as collagen, fibronectin and fibrillin give rise to large assemblies, which are organized into tissue-specific macrostructures, and therefore they inevitably interact with their own molecules, the other matrices, and cell surface receptors such as integrins and syndecans. As for collagen assembly, purified collagens could self-assemble into fibrils in the absence of cells, but the way in which *in vivo* collagens become organized into fibrillar matrices has been suggested to be under cellular control (Yamada et al., 2003). Indeed, *in vivo* assembly of collagen molecules is a multistep process (Trelstad, 1982) and fibroblasts exert controls over the steps from the molecules to fibrils, fibrils to fibers (fibril bundles), and fibers to tissue-specific 3D architecture. Birk and Trelstad (1984, 1986) demonstrated the presence of fibril channels and bundle-forming compartments ultrastructurally; that is, fibril polymerization occurs within narrow channels in the fibroblast surface, and fibril bundle formation occurs within a more peripheral extracytoplasmic compartment defined by a single or adjacent fibroblasts.

In fibronectin assembly, hierarchical steps for fibril, bundle and macroaggregate formation are not well demarcated, but cell involvement, or an integrin-dependent process on the cell surface, is known to be essential for conformational changes of extracellular fibronectin undergoing multimeric fibril formation (Schwarzbauer and Sechler, 1999; Mao and Schwarzbauer, 2005). Interestingly, pericellular fibronectin acts as a suitable template for fibrillin assembly. Kinsey et al. (2008) reported that α5β1-integrin-mediated fibronectin fibrillogenesis regulates fibrillin assembly into microfibrils in the pericellular milieu. Tsuruga et al. (2009) showed by antagonistic inhibition that integrin αvβ3 is involved in control over the fibrillin-1 deposition at the cellular level. In addition, Massam-Wu et al. (2010) reported that not only integrins but syndecan affect pericellular assembly of fibrillin and related molecules, and thus regulate TGFβ bioavailability. These studies indicate the significance of cellular activity in the primary step for both fibronectin and fibrillin assemblies. Meanwhile, in oxytalan fiber formation, the primary step for molecule to fiber need to be followed by a discrete next step, in which fibrillin microfibrils with a distinct diameter are organized into fibril bundles (or oxytalan fibers), but unlike being shown in bundle formation of collagen fibrils, *in vivo* progression of microfibril to the bundle has, so far, not been examined in detail.

To explore this issue, the present study was undertaken to investigate the development of oxytalan fibers in the chick presumptive dermis at the ultrastructural level. Bundle formation of fibrillin microfibrils could take place in elastic and nonelastic tissues. Adult dermis is an elastic-type tissue, but our previous studies showed that elastin deposition on microfibril bundles occurs only at later than embryonic Day 13 in the presumptive dermis of leg bud autopod (Yamazaki et al., 2007a). In addition, those microfibril bundles, or oxytalan fibers, are arranged in a unique spaced parallel array originating perpendicularly from the dermoepidermal junction (Isokawa et al., 2004). A distinct parallel orientation of the developing bundles without elastin deposition is greatly beneficial to the examination in this study. Using this embryonic chick autopod model, we demonstrate *in vivo* oxytalan fiber formation taken place through the increase of constitutive microfibrils in number under the close association of mesenchymal cell surface with some membrane specification.

MATERIALS AND METHODS

Preparation of Specimens

Fertilized eggs of White Leghorn (*Gallus gallus*) obtained from a local hatchery (Oohata Shaver, Shizuoka) were incubated at 39°C in a humidified incubator (MTI-201A; EYELA). Embryos at stages 24, 27, and 29 were selected according to the morphological criteria by Hamburger and Hamilton (1951) and denoted in embryonic days (ED), that is, ED4, 5, and 6, respectively. Embryos (n = 18 each for ED4-6) for histological and ultrastructural observations were fixed in 2.5% glutaraldehyde (GA) in phosphate-buffered saline (pH 7.35; PBS) for 2 hr at 4°C, and those (n = 30, 40, 20 for ED4-6) for immunohistochemical staining were fixed in 4% paraformaldehyde (PFA) in PBS for 2 hr at 4°C. Hind limb buds excised from aldehyde-fixed embryos were used as specimen. All the procedures were carried out in accordance with a guideline by the Animal Experimentation Committee of Nihon University School of Dentistry, which is in compliance with the Nation Act on Welfare and Management of Animals.

Histological Observation

Limb bud specimens fixed in GA were postfixed in 1% OsO_4 in 0.1 M phosphate buffer (pH 7.3) for 2 hr at room temperature, dehydrated in graded ethanols and propylene oxide, and embedded in Spurr's resin (1969), from which 0.8-μm-thick sections of the presumptive dermis were prepared tangentially to its ectodermal covering. Approximately 60% of specimens were sectioned tangentially and the rest longitudinally along the proximodistal axis of the limb bud. The sections were stained with 1% toluidine blue containing 1% sodium borate and examined under a microscope (Vanox, AH-2; Olympus) equipped with a digital camera (DP11; Olympus).

Immunohistochemistry

Limb bud specimens fixed in PFA were processed for immunohistochemistry as reported previously (Isokawa et al., 1994). Briefly, they were immersed in a graded series of sucrose (10%, 15%, and 20%) in PBS for cryoprotection, embedded in Tissue-Tek OCT compound (Miles), and frozen in liquid nitrogen-cooled 2-methyl butane. Approximately 90% of specimens were cryosectioned tangentially to the covering ectoderm and the rest longitudinally along the proximodistal axis of the limb bud. The cryosections, 7 μm in thickness, were equilibrated in PBS for 10 min and treated with 1% bovine serum albumin (BSA) in PBS for 1 hr. Subsequently, the sections were reacted with primary antibodies for 1 hr at room temperature, rinsed in PBS, and then incubated in a 1:100 dilution of fluorescein-isothiocyanate (FITC)-conjugated secondary antibody (ICN Pharmaceuticals, CA) in 1% BSA-PBS for 1 hr at room temperature. The sections were rinsed in PBS, and mounted with SlowFade™ (Light Antifade Kit; Molecular Probes). Controls included the omission of primary antibodies or the use of nonimmune IgG for the primary antibody incubation. Observations were carried out with

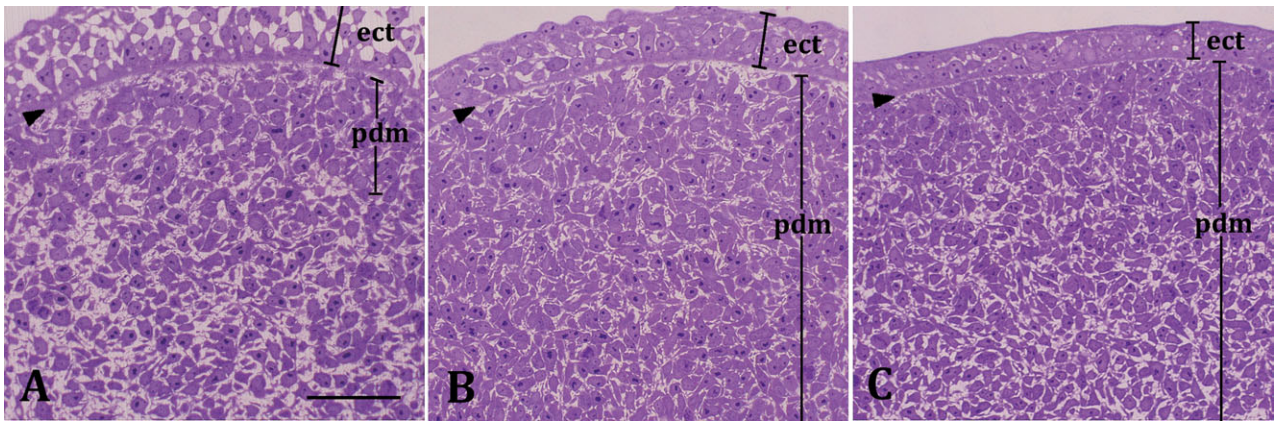

Fig. 1. Tangentially prepared, histological sections through the limb bud presumptive dermis (pdm) at ED4 (**A**), ED 5 (**B**), and ED6 (**C**). Plastic embedded leg bud tissue was sectioned and stained with toluidine blue. Arrowheads indicate a boundary basement membrane between "pdm" and the ectodermal cell layer (ect). All panels are presented in the same magnification and a scale bar in A is 30 μm.

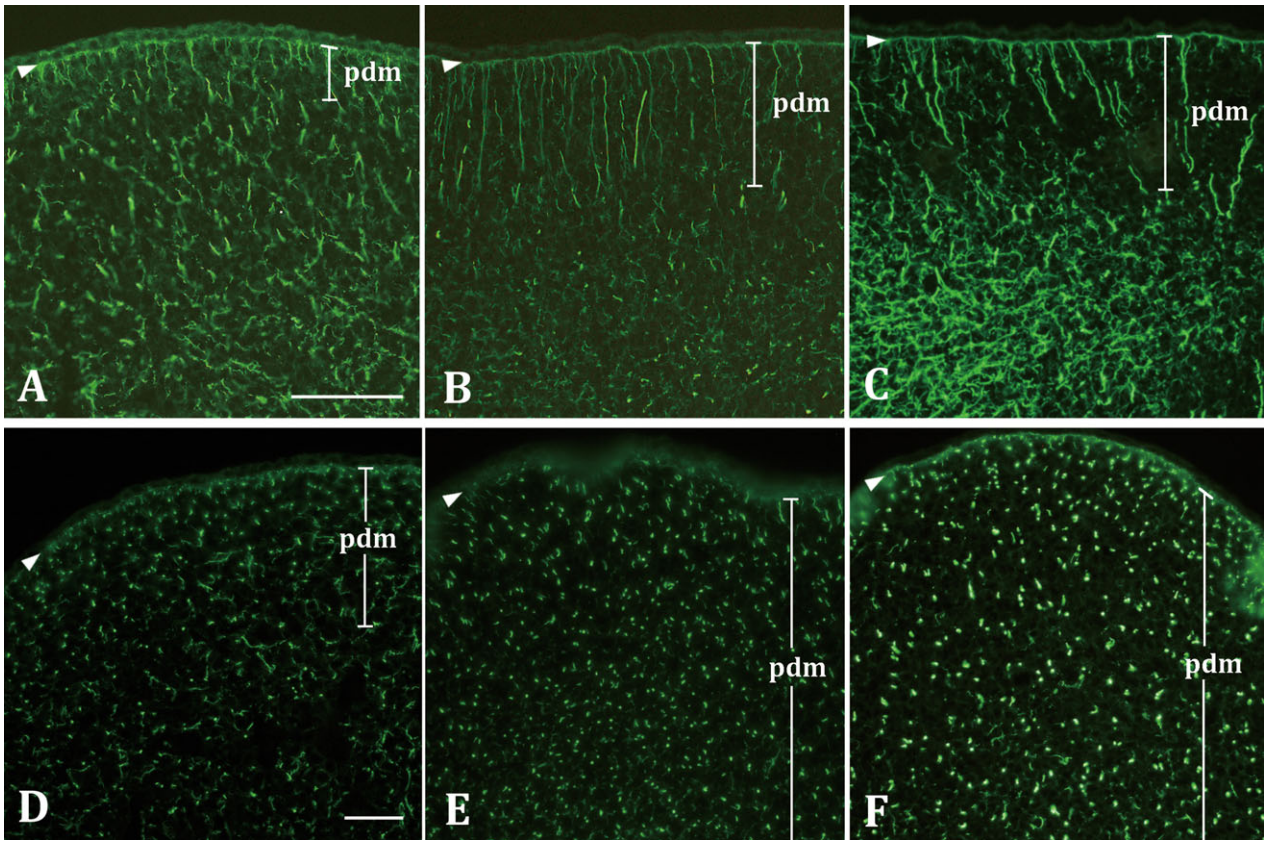

Fig. 2. Aldehyde-fixed frozen sections immunostained with anti-fibrillin-2. Presumptive dermis (pdm) and the overlaying ectodermal cell layer are shown at ED4 (**A**, **D**), ED5 (**B**, **E**) and ED6 (**C**, **F**) in the limb bud sections along a proximodistal axis (A–C; a scale bar in A is 30 μm) and in tangential sections through "pdm" (D–F; a bar in D is 30 μm). Arrowheads indicate the basement membrane beneath an ectodermal cell layer.

an epifluorescence microscope (Eclipse E600; Nikon) equipped with a CCD camera (Pro 600ES; Pixera).

All of primary antibodies used in this study were directed to avian antigens. Undiluted conditioned medium collected from culture of FB1 hybridoma (Isokawa et al., 2004) was used for fibrillin staining. Monoclonal antibodies (1:100 dilution in use) to integrin β1 (CSAT; Neff et al., 1982), α5 (A21F7; Muschler and Horwitz, 1991), and α6 (P2C62C4; Bronner-Fraser et al., 1992) were obtained from the Developmental Studies Hybridoma Bank

(University of Iowa, Iowa City, IA). Monoclonal antibody to αvβ3 (LM609; Cheresh and Spiro, 1987) and polyclonal antibody to fibronectin (AB1946; Yamada, 1983) were purchased from Chemicon International.

Electron Microscopy

Ultrathin sections, 75 nm in thickness, were prepared from resin embedded specimens, identical to those served for histological observations in toluidine blue-stained sections. The sections were contrasted with uranyl acetate and lead (Hanaichi et al., 1986), and examined in a Hitachi H-800 transmission electron microscope at an accelerating voltage of 75 kV. Some (n = 5 each for ED4-6) of the osmicated leg bud specimens were fractured with a razor blade, dehydrated in graded ethanols and critical-point-dried with isoamyl acetate and CO_2 as the transitional and exchange fluids, respectively (HCP-2; Hitachi). The dried specimens were coated in an osmium coater (HPC-1S; Vacuum Device, Ibaraki, Japan) for 20 sec and observed with a Hitachi S-4300 field emission-type scanning electron microscope (SEM) operated at 15 kV.

Histomorphometry

At the light microscopic level, immunofluorescence micrographs from tangential sections stained for fibrillin were used for histomorphometry. Three micrographs derived from different embryos were randomly selected at each of ED4-6. In each of selected micrographs, the number of stained fibers and the cross-section area of individual fiber were measured in unoverlapped three areas (50 × 50 μm^2 each), using an image software (ImageJ, ver. 1.44f; U.S. National Institutes of Health).

At the electron microscopic level, electron micrographs (45,000×; taken at 18,000× and printed at 2.5×) were used. Orthogonally sectioned oxytalan fibers (i.e., microfibril bundles) with a clearer resolution were randomly selected (n = 8 each at ED4 and 5, n = 4 at ED6). The number of microfibrils in each oxytalan fiber was counted manually with a magnifying glass.

Values are presented as mean ± standard errors and statistically analyzed by Student's t test with Holm's adjustment utilizing R (ver.2.10.0; R Foundation for Statistical Computing, Austria).

RESULTS

Tangential sections through the presumptive dermis of chick limb bud at ED4-6 showed a mesodermal tissue densely populated by mesenchymal cells (Fig. 1). In these sections, individual extracellular fibers could be hardly observed and most of the stained materials in the intercellular space were cytoplasmic processes when examined at the ultrastructural level (as described below). However, a well-oriented organization of oxytalan fibers in the presumptive dermis was successfully demonstrated by fibrillin immunohistochemistry (Fig. 2). Immunohistochemical preparations along the proximodistal axis of a limb bud showed that fibrillin-positive fibers originating perpendicularly from the basement membrane were extended into the presumptive dermis (Fig. 2A–C); the fibers at ED4 were shorter and those at ED5-6 longer. These fibers were observed as numerous fibrillin-positive dots in tangential sections (Fig. 2D–F). Dots represent the cross-sectioned

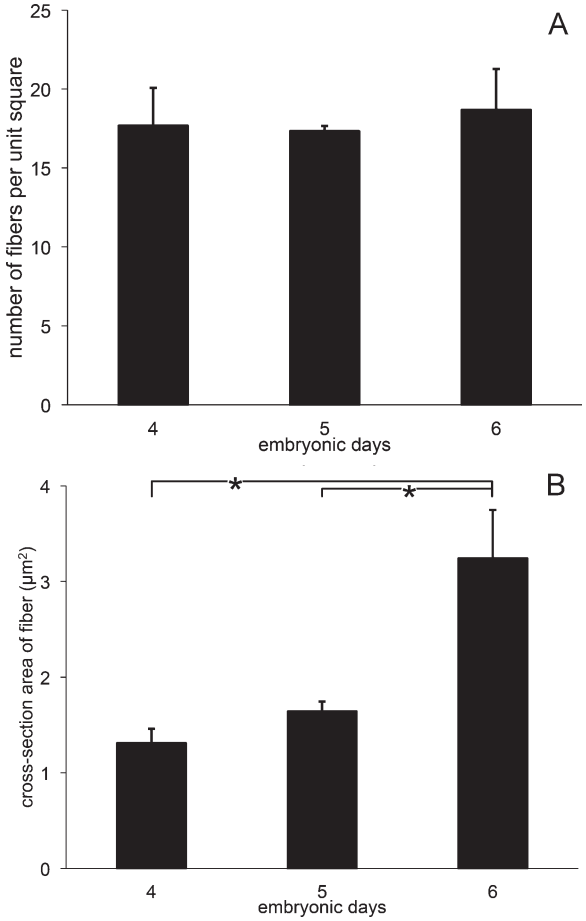

Fig. 3. The number of fibrillin-positive fibers in 50-μm^2 areas (**A**) and cross-section area of fibers (**B**) in the presumptive dermis at ED4, 5, and 6. Results are expressed as mean ± standard errors (n = 9); *$P < 0.01$.

surface of individual fibers and it was quantitatively confirmed that dots at ED6 were larger in size than those at ED4 or 5, while the number of dots, or fibers, in a unit area remained relatively constant during ED4-6 (Fig. 3).

Ultrastructurally, each of the oxytalan fibers was shown as a collection of an increasing number of tubular-appearing microfibrils (Fig. 4). The number of microfibrils per fiber increased approximately fourfold from ED4 to 5 and threefold from ED5 to 6 (Fig. 5); precisely, the number was 14.8 ± 1.2 (mean ± SE; n = 8) at ED4, 69.8 ± 12.9 (n = 8) at ED5 and 202.5 ± 42.1 (n = 4) at ED6. An average diameter of individual microfibrils remained constant, being 14.1 ± 0.9 nm (n = 70). In the stages examined (ED4-6), oxytalan fibers were observed in the close vicinity of mesenchymal cells (Fig. 4E). Thin fibers at ED4-5 sit mostly on a plain cell surface, frequently being cradled between such surfaces of two different cells (Fig. 4A,C). Thicker fibers at ED5-6 tended to be held in a shallow ditch on the cell surface or in a deeper furrow generated by lamellipodial protrusion (Figs. 4D, F–H, and 6). At the sites close to oxytalan fibers, plasmalemma and its undercoat showed a thickening with increased electron density. In addition, microfibrils in the periphery of oxytalan fibers appeared

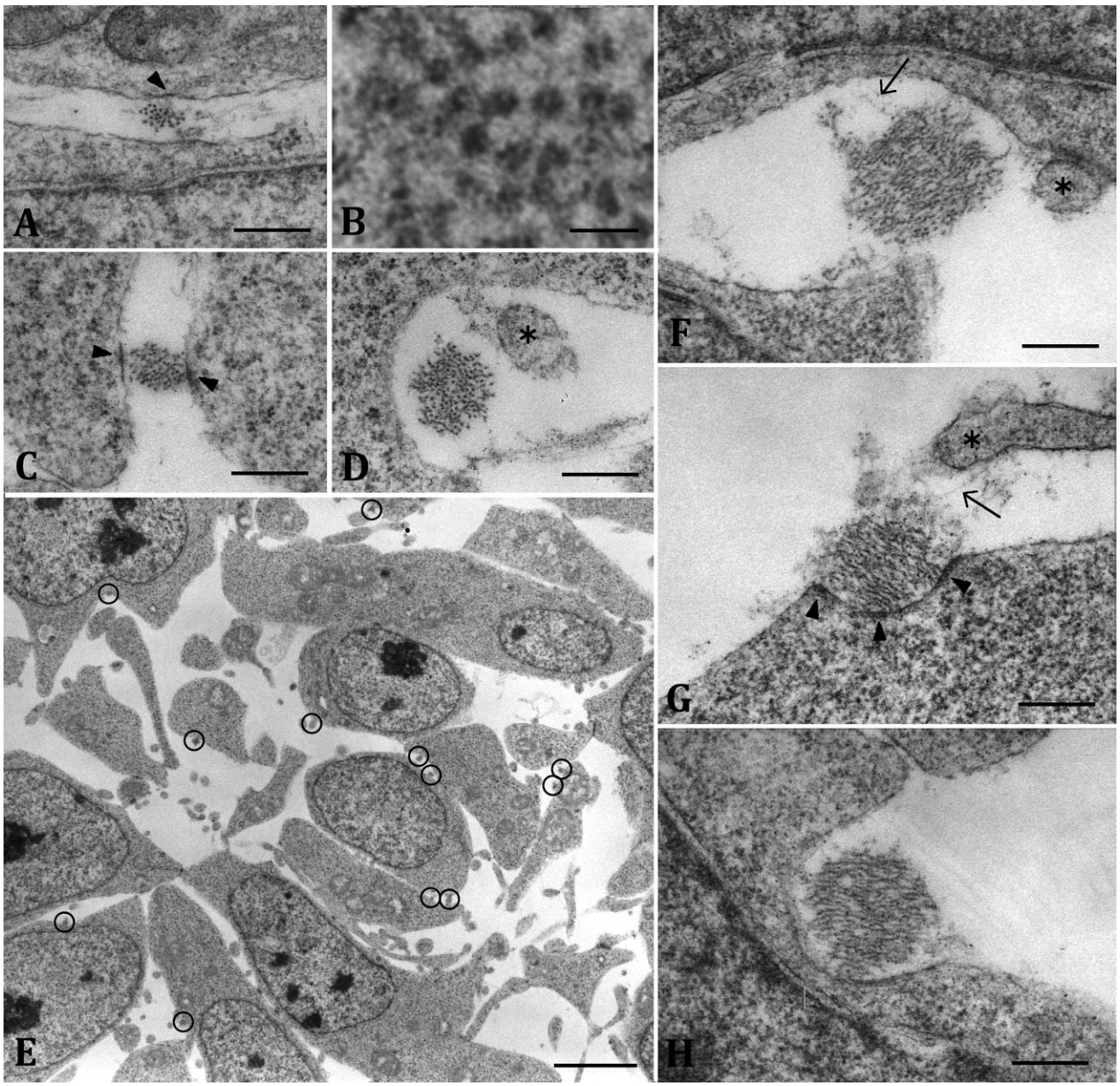

Fig. 4. Cross-sectioned images of oxytalan fibers observed in ultrathin sections prepared tangentially through the presumptive dermis at ED4 (**A**), ED5 (**B**–**E**), and ED6 (**F**–**H**). Panels except for B and E are all presented in the same magnification and scale bars are 0.3 μm. At high magnification (B; bar = 0.03 μm), tubular appearance of microfibrils is shown. A low magnification image (E; bar = 3 μm) demonstrates that oxytalan fibers (encircled) are preferentially situated in the close vicinity of cells. Arrowheads in A, C, and G indicate a membrane thickening with higher electron density at the cell surface facing oxytalan fibers. Arrows in F and G indicate flocculent strands connecting an oxytalan fiber and a nearby cell membrane. Asterisks in D, F and G indicate cytoplasmic processes of mesenchymal cells.

to adhere directly or by means of short flocculent strands to a nearby cell membrane. These observations in the cross sectioned images of oxytalan fibers were confirmed by examining longitudinally sectioned fibers (Fig. 7). Namely, microfibrils adhering to the cell membrane showed an apparent outward bowing at the sites of cell–fibril adhesion, and, on the other hand, a corresponding cell surface bulged out slightly toward the bowing of microfibrils in the periphery of oxytalan fibers. In these sites, microfibrils were attached closely to the bulged cell surface or tied by means of flocculent strands to a nearby cell membrane.

Immunohistochemical staining at the light microscopic level showed that β1, α5, and αvβ3 integrins were positive in mesenchymal cells in the presumptive dermis at ED5, while no specific staining was observed for α6 integrin and in the control in which primary antibodies were omitted (Fig. 8). Positive staining for fibronectin appeared extracellularly, and it delineated crowded cells in the presumptive dermis (Fig. 8E).

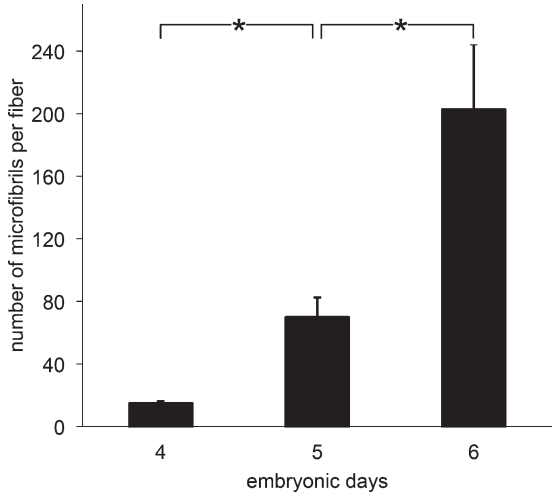

Fig. 5. Number of microfibrils in single oxytalan fibers in the presumptive dermis at ED4, 5, and 6. Results are expressed as mean ± standard errors (n = 8 at ED4 and 5, n = 4 at ED6); *$P < 0.01$.

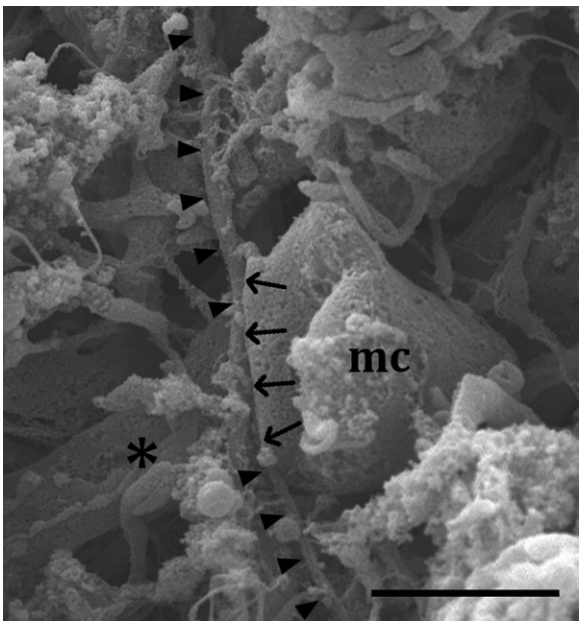

Fig. 6. Scanning electron micrograph of an oxytalan fiber in the presumptive dermis at ED6. A fiber indicated by arrowheads is held in a relatively deep ditch generated by lamellipodial protrusion (arrows) of a mesenchymal cell (mc) with a thick cytoplasmic process (asterisk). A scale bar represents 3 μm.

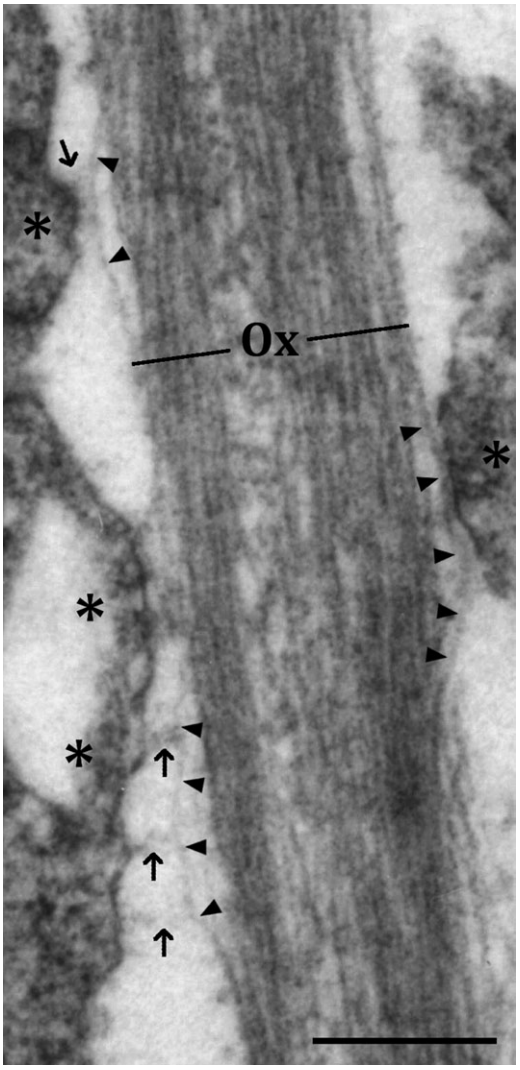

Fig. 7. Longitudinally sectioned image of an oxytalan fibers in the presumptive dermis at ED6. Outward bowing (arrowheads) of microfibrils is shown in the periphery of an oxytalan fiber (Ox). Those microfibrils are associated closely to the bulged cell surface or tied by means of flocculent strands (arrows) to a nearby cell membrane. Asterisks indicate the bulge region of cell surface with higher electron density in its plasmalemma and undercoat. A scale bar represents 0.3 μm.

DISCUSSION

We showed histomorphometrically that the thickness of oxytalan fibers in the presumptive dermis increased as their formation proceeded from ED4 to 6 in the chick autopod model. The increase of thickness appeared to be attained by incorporating newly formed microfibrils into preexisting bundles of fewer microfibrils, because the number of microfibrils per one bundle increased significantly at the ultrastructural level (Fig. 5), while the number of bundles (oxytalan fibers) remained almost constant (Figs. 2D–F and 3A). Cell to fiber ratio at ED6 would be ~2:1, when estimated by the present data (18.7 fibers in 50-μm^2 area; Fig. 3A) and our previous data (23.3 cells in 40-μm^2 area; Yamazaki et al., 2012). The possibility that a thicker fiber is formed by combining more than two thinner fibers together cannot be excluded completely and we indeed observed such cases in oxytalan fiber formation in the ED10-chick gizzard (unpublished data). However, in the early stages of the limb autopod development focused on in this study, we could not find any such ultrastructural images indicating the merging of thinner fibers. It is therefore considered that *de novo* assembly of microfibrils was active in the periphery of and/or deep within the preexisting bundles in the early stages, or ED4-6. This explanation is consistent with our

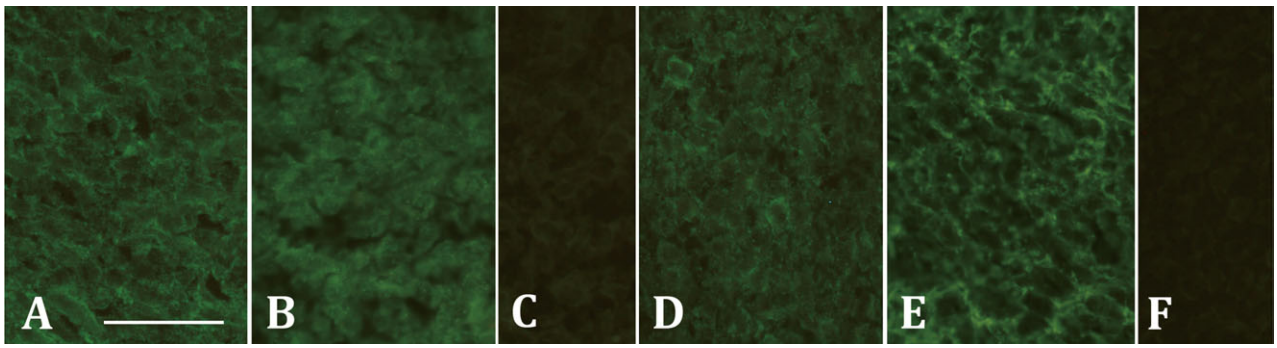

Fig. 8. Aldehyde-fixed frozen sections of ED5-presumptive dermis immunostained for integrins and fibronectin. Immunoreactivities for integrin β1 by CSAT (**A**), α5 by A21F7 (**B**), α6 by P2C62C4 (**C**) and αvβ3 by LM609 (**D**) and for fibronectin by AB1946 (**E**) are shown. No specific staining is observed in C and in the control (**F**), in the latter primary antibodies are omitted. All panels are presented in the same magnification and a scale bar in A is 30 μm.

previous finding that mesenchymal cells prepared from limb bud mesoderm at early stages of development are the potent producer of fibrillin and form a microfibrillar network *in vitro* (Yamazaki et al., 2007b).

In this study, we also showed an ultrastructurally discernible adhesion between a developing bundle of microfibrils and mesenchymal cell surface. "Outward bowing" of peripheral microfibrils and a corresponding "bulging" of cell surface (Fig. 7) may actually be artifacts due to shrinkage in tissue preparation for electron microscopy. Even in that case, these instead indicate a relatively stable adherence of cells to peripheral microfibrils of oxytalan fibers. This interpretation is endorsed by the observed characteristic membrane specification (i.e., membrane thickening and its undercoat with increased electron density) at sites of cell–fiber adhesion. In this context, occasional flocculent strands between oxytalan fibers and a nearby cell membrane might be also artifactual structure caused by peeling-off force in tissue shrinkage, but these strands again suggest the presence of protein complex such as integrins (Bax et al., 2003; Jovanović et al., 2008; Tsuruga et al., 2009), fibronectin (Mao and Schwarzbauer, 2005; Massam-Wu et al., 2010), fibrillins (Ramirez and Sakai, 2010; Sengle et al., 2012) and associated extracellular molecules (Hirai et al., 2007; Segade, 2009; Todorovic and Rifkin, 2012) at the sites of cell–fiber adhesion. Although we have been so far unable to determine convincingly their immunohistochemical identity at the ultrastructural level, our immunohistochemical survey at the light microscopic level suggested that β1, α5 and αvβ3 integrins and fibronectin are good candidates for the molecules constituting a cell to fiber-connecting structure observed in this study.

Cell–fiber adhesion observed in this study might represent the sites for *de novo* assembly of microfibrils, as alluded by previous *in vitro* studies (Kinsey et al., 2008; Massam-Wu et al., 2010). If this is the case, the increase in the thickness of (and in the number of microfibrils in) oxytalan fibers occurs in the surface of the fibers. However, new microfibrils could also be assembled from fibrillins diffused into deep within preexisting bundles of microfibrils, because it is known that elastin molecules are successfully deposited in the core of microfibril bundle served to elaunin and elastic fiber formation (Ross, 1973; Isokawa et al., 1990). Therefore, microfibril assembly in these two sites (the surface and deep within the bundles) is not mutually exclusive and, if cells and their protrusions try to render extracytoplasmic compartments for partitioning smaller extracellular milieu, both types of microfibril assembly is likely to be facilitated.

In collagen fiber formation in the chick cornea, tendon and dermis (Birk and Trelstad, 1984, 1986; Ploetz et al., 1991), there are known distinct cellular devices such as a narrow fibril-forming channel and a wider bundle-forming extracytoplasmic compartment, which are shapened by the changes of cell surface morphology and cell processes. In this present study focused on microfibril bundle, we described shallow "ditches" and deeper "furrows." We must say that they appeared crude and apparently less efficient in partitioning small extracellular milieu than the reported counterparts for collagen fibers. Ploetz et al. (1991) reported their observations in dorsolateral trunk dermal tissue at ED15 and we showed those in limb bud autopod dermal tissue at ED4-6. However, the crudeness of "ditches" and "furrows" in our observations was not simply due to the developmental stages but a much more likely to arise from the differences of fibril species (i.e., collagen fibrils vs. fibrillin microfibrils) in which cells and their devices are involved. Microfibril bundles are the primary (and precocious) fibrous system in the presumptive dermis of chick limb bud before the development of robust collagen fibers in dermis (Isokawa et al., 2004; Yamazaki et al., 2007a). It may be therefore feasible to interpret that morphologically crude "ditches" and "furrows" were in a primitive form devised for bundling fibrillin microfibrils into oxytalan fibers in chick presumptive dermis. From this point of view, our findings can be concluded in that the bundling of fibrillin microfibrils into oxytalan fibers is a progressive and closely cell-associated process.

ACKNOWLEDGEMENT

The authors thank Hideo Nagai for his technical assistance in scanning electron microscopy.

LITERATURE CITED

Bax DV, Bernard SE, Lomas A, Morgan A, Humphries J, Shuttleworth CA, Humphries MJ, Kielty CM. 2003. Cell adhesion to

fibrillin-1 molecules and microfibrils is mediated by α5β1 and αvβ3 integrins. J Biol Chem 278:34605–34616.
Birk DE, Trelstad RL. 1984. Extracellular compartments in matrix morphogenesis: collagen fibril, bundle, and lamellar formation by corneal fibroblasts. J Cell Biol 99:2024–2033.
Birk DE, Trelstad RL. 1986. Extracellular compartments in tendon morphogenesis: collagen fibril, bundle, and macroaggregate formation. J Cell Biol 103:231–240.
Bronner-Fraser M, Artinger M, Muschler J, Horwitz AF. 1992. Developmentally regulated expression of α6 integrin in avian embryos. Development 115:197–211.
Cheresh DA, Spiro RC. 1987. Biosynthetic and functional properties of an Arg-Gly-Asp-directed receptor involved in human melanoma cell attachment to vitronectin, fibrinogen, and von Willebrand factor. J Biol Chem 262:17703–17711.
Hamburger V, Hamilton HL. 1951. A series of normal stages in the development of the chick embryo. J Morphol 88:49–92.
Hanaichi T, Sato T, Iwamoto T, Malavasi-Yamashiro J, Hoshino M, Mizuno N. 1986. A stable lead by modification of Sato's method. J Electron Microsc (Tokyo) 35:304–306.
Hirai M, Horiguchi M, Ohbayashi T, Kita T, Chien KR, Nakamura T. 2007. Latent TGF-β-binding protein 2 binds to DANCE/fibulin-5 and regulates elastic fiber assembly. EMBO J 26: 3283–3295.
Hurle JM, Hinchliffe JR, Ros MA, Critchlow MA, Genis-Galvez JM. 1989. The extracellular matrix architecture relating to myotendinous pattern formation in the distal part of the developing chick limb: an ultrastructural, histochemical and immunocytochemical analysis. Cell Differ Dev 27:103–120.
Isokawa K, Rezaee M, Wunsch A, Markwald RR, Krug EL. 1994. Identification of transferrin as one of multiple EDTA-extractable extracellular proteins involved in early chick heart morphogenesis. J Cell Biochem 54:207–218.
Isokawa K, Sejima H, Shimizu O, Yamazaki Y, Yamamoto K, Toda Y. 2004. Subectodermal microfibrillar bundles are organized into a distinct parallel array in the developing chick limb bud. Anat Rec A Discov Mol Cell Evol Biol 279:708–719.
Isokawa K, Takagi M, Toda Y. 1990. Ultrastructural and cytochemical study of elastic fibers in the ventral aorta of a teleost, *Anguilla japonica*. Anat Rec 226:18–26.
Jovanović J, Iqbal S, Jensen S, Mardon H, Handford P. 2008. Fibrillin-integrin interactions in health and disease. Biochem Soc Trans 36:257–262.
Kielty CM, Sherratt MJ, Shuttleworth CA. 2002. Elastic fibres. J Cell Sci 115:2817–2828.
Kinsey R, Williamson MR, Chaudhry S, Mellody KT, McGovern A, Takahashi S, Shuttleworth CA, Kielty CM. 2008. Fibrillin-1 microfibril deposition is dependent on fibronectin assembly. J Cell Sci 121:2696–2704.
Mao Y, Schwarzbauer JE. 2005. Fibronectin fibrillogenesis, a cell-mediated matrix assembly process. Matrix Biol 24:389–399.
Massam-Wu T, Chiu M, Choudhury R, Chaudhry SS, Baldwin AK, McGovern A, Baldock C, Shuttleworth CA, Kielty CM. 2010. Assembly of fibrillin microfibrils governs extracellular deposition of latent TGFβ. J Cell Sci 123:3006–3018.
Muschler JL, Horwitz AF. 1991. Down-regulation of the chicken α5β1 integrin fibronectin receptor during development. Development 113:327–337.
Neff NT, Lowrey C, Decker C, Tovar A, Damsky C, Buck C, Horwitz AF. 1982. A monoclonal antibody detaches embryonic skeletal muscle from extracellular matrices. J Cell Biol 95:654–666.
Ploetz C, Zycband EI, Birk DE. 1991. Collagen fibril assembly and deposition in the developing dermis: segmental deposition in extracellular compartments. J Struct Biol 106:73–81.
Ramirez F, Sakai LY. 2010. Biogenesis and function of fibrillin assemblies. Cell Tissue Res 339:71–82.
Ross R. 1973. The elastic fiber. J Histochem Cytochem 21:199–208.
Schwarzbauer JE, Sechler JL. 1999. Fibronectin fibrillogenesis: a paradigm for extracellular matrix assembly. Curr Opin Cell Biol 11:622–627.
Segade F. 2009. Functional evolution of the microfibril-associated glycoproteins. Gene 439:43–54.
Sengle G, Tsutsui K, Keene DR, Tufa SF, Carlson EJ, Charbonneau NL, Ono RN, Sasaki T, Wirtz MK, Samples JR, Fessler LI, Fessler JH, Sekiguchi K, Hayflick SJ, Sakai LY. 2012. Microenvironmental regulation by fibrillin-1. PLoS Genet 8:e1002425.
Spurr AR. 1969. A low-viscosity epoxy resin embedding medium for electron microscopy. J Ultrastruct Res 26:31–43.
Todorovic V, Rifkin DB. 2012. LTBPs, more than just an escort service. J Cell Biochem 113:410–418.
Trelstad RL. 1982. Multistep assembly of type I collagen fibrils. Cell 28:197–198.
Tsuruga E, Sato A, Ueki T, Nakashima K, Nakatomi Y, Ishikawa H, Yajima T, Sawa Y. 2009. Integrin αvβ3 regulates microfibril assembly in human periodontal ligament cells. Tissue Cell 41: 85–89.
Yamada KM. 1983. Cell surface interactions with extracellular materials. Ann Rev Biochem 52:761–799.
Yamada KM, Pankov R, Cukierman E. 2003. Dimensions and dynamics in integrin function. Braz J Med Biol Res 36:959–966.
Yamazaki Y, Mikami Y, Yuguchi M, Namba Y, Isokawa K. 2012. Development of collagen fibres and Lysyl oxidase expression in the presumptive dermis of chick limb bud. Anat Histol Embryol 41:68–74.
Yamazaki Y, Sejima H, Yuguchi M, Namba Y, Isokawa K. 2007a. Late deposition of elastin to vertical microfibrillar fibers in the presumptive dermis of the chick embryonic tarsometatarsus. Anat Rec 290:1300–1308.
Yamazaki Y, Sejima H, Yuguchi M, Shinozuka K, Isokawa K. 2007b. Cellular origin of microfibrils explored by monensin-induced perturbation of secretory activity in embryonic primary cultures. J Oral Sci 49:107–114.